Event–Driven Prony: Towards Asynchronous Spectral Estimation

3 authors:

Ruiming Guo
Imperial College London
31 PUBLICATIONS **242** CITATIONS

SEE PROFILE

Yuliang Zhu
Imperial College London
5 PUBLICATIONS **27** CITATIONS

SEE PROFILE

Ayush Bhandari
Massachusetts Institute of Technology
123 PUBLICATIONS **2,889** CITATIONS

SEE PROFILE

Event-Driven Prony: Towards Asynchronous Spectral Estimation

Ruiming Guo, Yuliang Zhu and Ayush Bhandari

Dept. of Electrical and Electronic Engg., Imperial College London, SW7 2AZ, UK.

{ruiming.guo,yuliang.zhu19,a.bhandari}@imperial.ac.uk

Abstract—Mainstream signal processing theory and methods are primarily designed for synchronous sampling architectures, where samples are captured at predefined time instants. While this fits well with Shannon's framework, in the absence of synchronous structure, even fundamental tools like filtering and convolution break down. Alternatively, event-driven or time-encoded sampling offers a more efficient method by capturing signals only when an event occurs. This approach, reminiscent of the "spiking neuron" behavior in the brain, can lead to low-power electronic implementations. Unlike Shannon's framework, measurements in this scheme are defined by asynchronous sampling, presenting unique challenges. One such open problem is performing spectral estimation from asynchronous samples. In this paper, we propose a novel approach that directly enables spectral estimation from asynchronous measurements. Empirically, our algorithm offers robust, high-resolution spectral information, with a lower sampling rate on trigger times. Beyond numerical experiments, we build an event-driven sampling hardware utilizing asynchronous sigma-delta modulators to validate our approach. These hardware experiments further demonstrate the robustness and practical applicability of our method.

Index Terms—Event-driven, nonuniform sampling, non-linear reconstruction, spectral estimation, time-encoded sampling.

I. INTRODUCTION

Event-Driven Sampling. How to represent a continuous-time signal as a discrete sequence is at the core of the current digital acquisition protocol. At the core of current digitalization technology, the well-known Shannon-Nyquist sampling scheme [1] represents a continuous-time, bandlimited signal based on its amplitude samples taken at or above the so-called Nyquist rate by utilizing a synchronous clock. On a different perspective, one can circumvent the synchronous setup and sample the signal only when there is an "event". This leads to an alternative sampling paradigm that is known by, EVENT-DRIVEN [2], TIME-ENCODED [3], [4], ASYNCHRONOUS [5]–[8], IRREGULAR [9], [10], SEND-ON-DELTA Sampling [11], [12], which has been widely studied due to its potential benefit of being power efficient.

Related Works. Current works on the event-driven sampling or EDS predominantly focus on bandlimited signal classes. Recently, several papers have started to consider time-domain sparse signals [13]–[16]. Apart from the bandlimited and sparse signal classes, another class of signals that plays a pivotal role in application areas is sum of sinusoids (SoS). The study on SoS can be traced to the second millennium BC, in the context of astronomy and cosmology. Dating back to Prony [17], the utility of spectra analysis has motivated the sub-field of the so-called *high-resolution frequency estimation*, which has been thoroughly studied in the 1970-1990s [18]–[23]. Despite their prevalence and importance, such signals have not been considered in the EDS literature. The main reasons can be attributed to the following aspects. Firstly, SoS can be interpreted as a specific case of bandlimited signals. However, this standpoint leads to suboptimal recovery since it does not leverage the parametric structure of the sinusoids, as shown in the experimental results in Section IV. Secondly, algorithmic approaches based on time-decoding [3] do not directly translate to parametric

signals [13]–[16], [24]. In this context, the consideration of sparse signals is only very recent and it is natural to consider time-domain sparse signals as a first prototype example. Finally, EDS ADCs are still not mainstream yet and hence, such hardware has not been deployed for practical problems such as direction-of-arrival (DOA) estimation that intrinsically requires spectral estimation.

In a different incarnation, spectral estimation via low-resolution sampling is also at the heart of one-bit quantized DOA estimation [25]. The difference being, in one-bit DOA estimation, permanent information loss occurs due to concurrent quantization on both *amplitude* and *time*; while, in EDS spectral estimation, exact parameter retrieval is still possible due to the *non-uniformly spaced trigger times*. However, how to achieve this direct parameter retrieval is particularly challenging, as the asynchronous sampling setup instigates a stalemate with conventional spectral estimation methods that typically rely on uniform sampling.

Contributions. In this paper, we present an event-driven spectral estimation method called **ED-Prony** via asynchronous sampling, that allow direct frequency estimation from the time-encoded measurements. Compared to the conventional sequential reconstruction (*i.e.* , signal recovery followed by frequency estimation), **ED-Prony** enables robust, super-resolved, sinusoidal parameter retrieval with lower sampling rate (trigger times). Our main contributions are as follows.

- We propose a novel algorithm that directly extracts the spectral information from the time-encoded measurements (see Algorithm 1). Our algorithmic machinery utilizes a *coarse-to-fine* strategy that deconstructs non-linear optimization problem into sparse approximation, which results in a computationally efficient implementation.
- As practical validation of event-driven sampling has been rarely reported in literature, the validity of designed algorithms in real-world scenarios remains unknown. To this end, we build EDS hardware utilizing asynchronous sigma-delta modulators (ASDM) to validate our approach, demonstrating the robustness and super-resolution capability of **ED-Prony** in real-world settings (see Section IV).
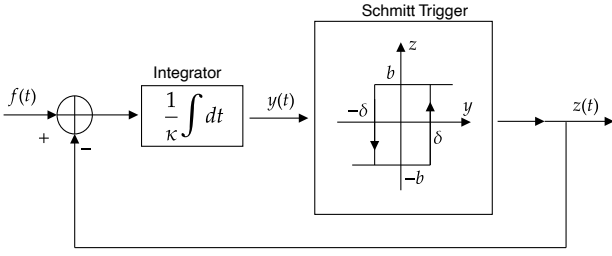
Notation. Integers, reals, and complex numbers are denoted by $\mathbb{Z}, \mathbb{R}$ and $\mathbb{C}$, respectively. We use $\mathbb{I}_N = \{0, \cdots, N-1\}, N \in \mathbb{Z}^+$ to denote the set of N contiguous integers. The indicator function on domain $\mathcal{D}$ is denoted by $\mathbb{1}_{\mathcal{D}}$. Continuous functions are written as $f(t), t \in \mathbb{R}$; their discrete counterparts are represented by $f[n] = f(t)|_{t=nT}, n \in \mathbb{Z}$. Continuous functions and discrete sequences are written as $f(t), t \in \mathbb{R}$ and $g[n]$, respectively. are written as ; their discrete counterparts are represented by $g[n] = g(t)|_{t=nT}, n \in \mathbb{Z}$ where $T = 2\pi/\omega_s > 0$ is the sampling period. Vectors and matrices are written in bold lowercase and uppercase fonts, *e.g.* $\mathbf{f} \in \mathbb{R}^N$ and $\mathbf{F} \in \mathbb{R}^{N \times M}$. The max-norm of a function is defined as, $\|f\|_\infty = \inf\{c_0 \geqslant 0 : |f(t)| \leqslant c_0\}$; for sequences, we use, $\|f\|_\infty = \max_n |f[n]|$. The ℓ_2-norm of a sequence is defined as $\|f\|_2 = (\sum_{n=0}^{N-1} |f[n]|^2)^{1/2}$.

II. EVENT-DRIVEN SAMPLING OF SUM OF SINUSOIDS

Problem Formulation. The EDS scheme used in this paper is depicted in Fig. 1, which encodes the amplitude information of the input signal $f(t)$ as a time sequence $\{t_n\}_{n \in \mathbb{Z}}$. The bounded input signal

(a) Block Diagram of the Event-Driven Sampling Paradigm.

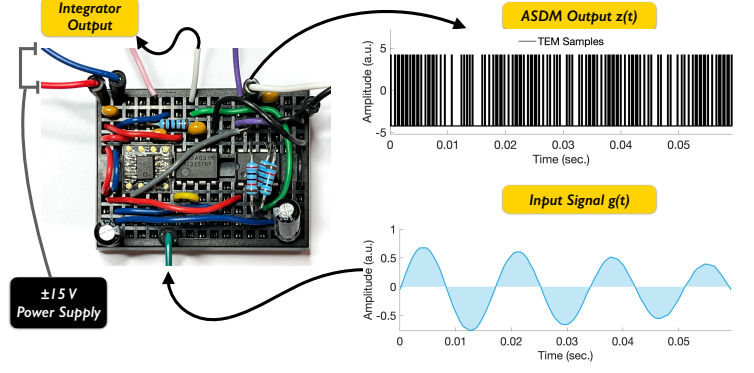(b) ASDM based Time Encoding Asynchronous Sigma-Delta Modulator

Fig. 1. The block diagram and hardware implementation of the EDS paradigm.

$f(t), |f(t)| \leqslant c < b$, is shifted by a constant amount $\pm b$ before being fed into the integrator. The bias b ensures that the integrator's output $y(t)$ is a positive (negative) increasing (decreasing) function of time. There are two possible operating modes in steady state. In the first mode, the output of the EDS is in state $z(t) = -b$ and the input to the Schmitt trigger increases from $-\delta$ to δ. When the output of the integrator reaches the maximum value δ, a transition of the output signal $z(t)$ from $-b$ to b is triggered and the feedback changes the sign (becomes negative). In the second mode, the EDS is in the state $z(t) = b$ and the integrator output decreases from δ to $-\delta$. When the minimum value $-\delta$ is achieved, $z(t)$ will reverse to $-b$. Thus, while the transition times of the output $z(t)$ are non-uniformly spaced, the modulus of $z(t)$ remains constant, *i.e.* $|z(t)| = b$. As a result, a transition of the output from $-b$ to b or vice-versa takes place every time the integrator output reaches the triggering threshold δ or $-\delta$. The time when this threshold is attained depends on $f(t)$ as well as on the design parameters κ, δ and b. The EDS maps amplitude information into timing information via a signal-dependent sampling paradigm.

In this paper, we focus on the sum of sinusoids (SoS) input

$$f(t) = \sum_{k=0}^{K-1} c_k e^{j\omega_k t}, \quad \Omega \overset{\text{def}}{=} \max_k |\omega_k| \quad (1)$$

which generates a sequence of time stamps $\{t_n\}_{n\in\mathbb{Z}}$. $\omega_k = 2\pi f_k, k \in \mathbb{I}_K$ are the frequencies of sinusoids. Given *noisy* non-uniformly spaced time sequence $\{t_n\}_{n\in\mathbb{Z}}$ from the EDS paradigm, our goal is to robustly retrieve the sinusoidal parameters $\{c_k, \omega_k\}_{k\in\mathbb{I}_K}$.

Spectral Estimation via Time-Decoding. As the input signal $f(t)$ is Ω-bandlimited, an intuitive approach to estimate sinusoidal parameters is sequential reconstruction, *i.e.* time-decoding (TDM) [2], [3] followed by spectral estimation [26]–[28]. We shall show this sequential reconstruction approach and state the recovery conditions.

Step # 1: Recovery of $f(t)$ via Time-Decoding.

As illustrated in the block diagram in Fig. 1 (a), the sequence of trigger times $\{t_n\}_{n\in\mathbb{Z}}$ is generated by the recursive equation

$$\int_{t_n}^{t_{n+1}} f(t) \, dt = (-1)^n \left[-b\left(t_{n+1} - t_n\right) + 2\kappa\delta \right]. \quad (2)$$

Without any loss of generality, a simple version of the EDS will be leveraged, assuming $|f(t)| \leqslant c < b = 1$ and $\kappa = 1/2$, leading to

$$\int_{t_n}^{t_{n+1}} f(t) \, dt = (-1)^n \left[\delta - t_{n+1} + t_n \right]. \quad (3)$$

From (3), we shall show that the density of trigger times is bounded:

Lemma 1. *For an arbitrary bounded signal $f(t)$ with $|f(t)| \leqslant c < 1$, the distance between consecutive trigger times t_n and t_{n+1} is bounded*

$$\frac{\delta}{1+c} \leqslant t_{n+1} - t_n \leqslant \frac{\delta}{1-c}.$$

Proof. With $|f(t)| \leqslant c < 1$, we know

$$-c(t_{n+1} - t_n) \leqslant \int_{t_n}^{t_{n+1}} f(t)dt \leqslant c(t_{n+1} - t_n).$$

By replacing the integral in (3) and solving for $t_{n+1} - t_n$, we obtain the desired result. $\qquad\square$

$f(t)$ can be recovered via a sequence of recursive functions: Denote by $f = f(t)$. Let the operator $\mathcal{A}$ be defined by

$$\mathcal{A}f = \sum_{n\in\mathbb{Z}} f(s_n)g_n(t), \; g_n(t) \overset{\text{def}}{=} \left(h_\Omega * \mathbb{1}_{[t_n, t_{n+1}]} \right)(t) \quad (4)$$

where $s_n = (t_{n+1} + t_n)/2$, and $h_\Omega(t) = \sin(\Omega t)/\pi t$. $\mathbb{1}_{\mathcal{D}}$ is the indicator function on domain $\mathcal{D}$. Let $f_m(t)$ be a sequence of bandlimited functions defined by the recursion

$$f_{m+1} = f_m + \mathcal{A}(f - f_m), m \in \mathbb{N}$$

with the initial condition $f_0 = \mathcal{A}f$. Then, $f(t)$ can be recovered from $\{t_n\}_{n\in\mathbb{Z}}$, as $\lim_{m\to\infty} f_m(t) = f(t)$, provided that, $\delta < \frac{(1-c)\pi}{\Omega}$.

Step # 2: Spectral Estimation via Prony's Method.

Once $f(t)$ is reconstructed, $\{\omega_k\}_{k\in\mathbb{I}_K}$ can be retrieved from a sequence of uniform samples $\{f(mT)\}_{m\mathbb{I}_M}$ via Prony's method [26], provided that $T < \pi/\Omega$ and $M \geqslant 2K$. Having $\{\omega_k\}_{k\in\mathbb{I}_K}$ known, $\{c_k\}_{k\in\mathbb{I}_K}$ can be obtained via solving a linear system of equations.

Remarks. Throughout this sequential reconstruction, we can find that:

i) The time-decoding mechanism solely leverages the *bandlimited-ness* of f, without considering its *sinusoidal structure*.

ii) Our core problem is *parameter estimation*, which requires a different solving strategy than that used for signal reconstruction.

As a result, the sequential reconstruction approach is likely to compromise the robustness and resolution on spectral estimation, leading to sub-optimal performance in real-world scenarios.

III. ED-Prony: EVENT-DRIVEN FREQUENCY ESTIMATION

To fit the essence of spectral estimation problem, in this paper, we propose an estimation method that enables direct sinusoidal parameter

estimation from the event-driven samples. The key idea here is that, sinusoidal structure in (1) allows for establishing a parametric model of the event-driven time sequences. Hence, utilizing a model-fitting method, the sinusoidal parameters can be robustly retrieved via solving a non-convex optimization problem.

Our starting point is the non-uniform measurements at the output of the integrator. Combining (1) and (3), we have

$$y[n] = \int_{t_n}^{t_{n+1}} f(t) \, dt \stackrel{(1)}{=} \sum_{k=0}^{K-1} \underline{c}_k \left(e^{j\omega_k t_{n+1}} - e^{j\omega_k t_n} \right) \quad (5)$$

where $n \in \mathbb{I}_N$ and $\underline{c}_k = \frac{c_k}{j\omega_k}, k \in \mathbb{I}_K$. Notice that, $\{y[n]\}_{n \in \mathbb{I}_N}$ can be calculated from the time sequence $\{t_n\}_{n \in \mathbb{I}_{N+1}}$

$$y[n] \stackrel{(3)}{=} (-1)^n \left[\delta - (t_{n+1} - t_n) \right] \quad (6)$$

which implicitly "encode" the sinusoidal parameters $\{c_k, \omega_k\}_{k \in \mathbb{I}_K}$.

Sparse Spectral Estimation from EDS Samples. (6) holds in noiseless case. In real-world scenarios, (5) translates to

$$y[n] = \sum_{k=0}^{K-1} \underline{c}_k \left(e^{j\omega_k t_{n+1}} - e^{j\omega_k t_n} \right) + \eta[n], \quad n \in \mathbb{I}_N \quad (7)$$

where η models noise and hardware imperfections. From hardware experiments (see Section IV), we have empirically identified that η is dominated by time quantization on $\{t_n\}_{n \in \mathbb{I}_{N+1}}$. Denote by Δt the quantization step on the time sequence, then η is bounded by

$$|\eta[n]| \leqslant \sigma_\eta \stackrel{\text{def}}{=} 4 \left\| \underline{c}_k \right\|_{\ell_1} \sin(\tfrac{\Omega \Delta t}{2}) \quad (8)$$

provided that $\Delta t \ll \frac{\pi}{\Omega}$, which holds naturally in practice. With (7) and (8), the direct spectral estimation problem can be posed as

$$\min_{\underline{c}_k, \omega_k} \quad \sum_{n=0}^{N-1} \left| y[n] - \sum_{k=0}^{K-1} \underline{c}_k \left(e^{j\omega_k t_{n+1}} - e^{j\omega_k t_n} \right) \right|^2. \quad (9)$$

The minimization in (9) is challenging, due to the structure of the setup. In order to tackle this problem, we opt for a *coarse-to-fine* strategy where the goal is to split (9) into two tractable sub-problems, *viz.* P1 that addresses on-grid estimation of $\{\omega_k\}_{k \in \mathbb{I}_K}$ via sparse recovery and P2 that attains off-grid spectral estimation via perturbation theory. We outline the details of this two-stage minimization as follows.

P1: **On-Grid Sparse Approximation** Since the objective function in (9) is highly non-linear and non-convex, the key insight here is to relax the original problem utilizing on-grid approximation. This allows for solving the relaxed problem via sparse recovery techniques: Let $\mathbf{p}(\omega) \in \mathbb{C}^N$ where $[\mathbf{p}(\omega)]_n = e^{j\omega t_{n+1}} - e^{j\omega t_n}$, hence, an approximate problem to (9) is given by

$$\boxed{\text{P1}} \quad \min_{\mathbf{c}} \quad \|\mathbf{c}\|_{\ell_1}, \text{ s.t. } \|\mathbf{y} - \mathbf{P}_I \mathbf{c}\|_2 \leqslant \sqrt{N} \sigma \quad (10)$$

where $\mathbf{P}_I = [\mathbf{p}(\omega_0), \cdots, \mathbf{p}(\omega_I)]$ and $\omega_i = \frac{2\Omega i - \Omega(I+1)}{I+1}, i \in \mathbb{I}_{I+1}$. Hence, the minimizer to (10), *i.e.* $\{\widetilde{\omega}_k\}_{k \in \mathbb{I}_K}$, offers a K-sparse solution that approximates the ground-truth frequencies $\{\omega_k\}_{k \in \mathbb{I}_K}$ up to an error bounded by the grid step $\frac{2\Omega}{I+1}$. (10) is a convex optimization problem and can be solved efficiently via methods such as LASSO.

P2: **Off-Grid Spectral Estimation via Perturbation** With initial estimates $\{\widetilde{\omega}_k\}_{k \in \mathbb{I}_K}$ known from solving (10), our next goal is to further refine $\{\widetilde{\omega}_k\}_{k \in \mathbb{I}_K}$ to reduce the on-grid approximation error. To this end, we leverage the perturbation method: Let $\omega_k = \widetilde{\omega}_k + \Delta\omega_k, |\Delta\omega_k| \leqslant \frac{2\Omega}{I+1}$. The perturbation term $\Delta\omega_k$ is sufficiently small, provided that I

Algorithm 1 Event-Driven Prony

Input: Time sequence $\{t_n\}_{n=0}^N$.
1: Compute the samples $\{y[n]\}_{n=0}^{N-1}$ via (6).
2: Compute $\{c_k^{[0]}, \omega_k^{[0]}\}_{k=0}^{K-1}$ via solving (10).
3: **for** m = 1 to max. iterations **do**
4:   Update $\widetilde{\underline{\mathbf{c}}}_k^{[m]}, \widetilde{\boldsymbol{\omega}}^{[m]}$ via solving (12).
5:   **if** (14) holds **then**
6:     Terminate all loops;
7:   **end if**
8: **end for**
Output: The sinusoidal parameters $\{c_k, \omega_k\}_{k \in \mathbb{I}_K}$.

---

is large enough. Hence, (7) translates to

$$\begin{aligned} y[n] &= \sum_{k=0}^{K-1} \underline{c}_k \left(e^{j(\widetilde{\omega}_k + \Delta\omega_k)t_{n+1}} - e^{j(\widetilde{\omega}_k + \Delta\omega_k)t_n} \right) + \eta[n] \\ &= \sum_{k=0}^{K-1} (j e^{j\widetilde{\omega}_k t_{n+1}} t_{n+1} - j e^{j\widetilde{\omega}_k t_n} t_n) \underline{c}_k \Delta\omega_k \\ &\quad + \sum_{k=0}^{K-1} (e^{j\widetilde{\omega}_k t_{n+1}} - e^{j\widetilde{\omega}_k t_n}) \underline{c}_k + o(\Delta\omega_k) + \eta[n]. \quad (11) \end{aligned}$$

Let $\mathbf{q}(\omega) \in \mathbb{C}^N$, $[\mathbf{q}(\omega)]_n = j e^{j\omega t_{n+1}} t_{n+1} - j e^{j\omega t_n} t_n$. As a result, the perturbations can be found by solving the following minimization

$$\boxed{\text{P2}} \quad \min_{\mathbf{c}, \mathbf{r}} \quad \|\mathbf{y} - \mathbf{P}_K \mathbf{c} - \mathbf{Q}\mathbf{r}\|_2^2 \quad (12)$$

where $\mathbf{P}_K = [\mathbf{p}(\omega_0), \cdots, \mathbf{p}(\omega_K - 1)]$, $\mathbf{Q} = [\mathbf{q}(\omega_0), \cdots, \mathbf{q}(\omega_K - 1)]$ and $\mathbf{r} = \mathbf{c} \odot \Delta\boldsymbol{\omega}$ ($\odot$ denotes Hadamard product operation). (12) is a least-squares problem that boils down to solving a linear system of equations, *i.e.* its closed-form solution is given by,

$$[\mathbf{c}^\top, \mathbf{r}^\top]^\top = ([\mathbf{P}_K, \mathbf{Q}]^{\mathsf{H}}[\mathbf{P}_K, \mathbf{Q}])^{-1}[\mathbf{P}_K, \mathbf{Q}]^{\mathsf{H}} \mathbf{y}.$$

Once $\Delta\boldsymbol{\omega}$ is obtained, we can update the frequency estimates via $\widetilde{\omega}_k \leftarrow \widetilde{\omega}_k + \Delta\omega_k, k \in \mathbb{I}_K$.

Convergence. The proposed event-driven spectral estimation algorithm (**ED-Prony**) is bound to converge to at least some local minimum point [29], since the minimization in (12) results in

$$\mathcal{J}\left(\widetilde{\underline{\mathbf{c}}}_k^{[m+1]}, \widetilde{\boldsymbol{\omega}}^{[m+1]} \right) \leqslant \mathcal{J}\left(\widetilde{\underline{\mathbf{c}}}_k^{[m]}, \widetilde{\boldsymbol{\omega}}^{[m]} \right) \quad (13)$$

where $\mathcal{J}\left(\widetilde{\underline{\mathbf{c}}}_k^{[m]}, \widetilde{\boldsymbol{\omega}}^{[m]} \right) = \left\| \mathbf{y} - \mathbf{P}_K \widetilde{\underline{\mathbf{c}}}_k^{[m]} \right\|_2$. The **ED-Prony** algorithm converges in a few steps if the separation between any two frequencies is sufficiently large. We keep iterating the frequency refinement via solving (12) until the following criterion is satisfied

$$\|\mathbf{y} - \mathbf{P}_K \mathbf{c}\|_2 \leqslant \sqrt{N} \sigma \quad \text{(Stopping Criterion).} \quad (14)$$

In other words, in the presence of distortions such as quantization and noise, we can only retrieve $\{c_k, \omega_k\}_{k \in \mathbb{I}_K}$ up to a tolerance level of σ_η. The algorithmic procedure is summarized in Algorithm 1.

IV. NUMERICAL AND HARDWARE EXPERIMENTS

The overarching goal of our experiments is to validate the robustness and super-resolution capability of the proposed **ED-Prony** approach, utilizing lower sampling rate on trigger time sequence. In particular, through a series of 6 experiments, we show that the spectral information can be directly retrieved from the event-driven trigger times. Utilizing an asynchronous sigma–delta modulation implementation, we demonstrate frequency super-resolution up to 2 Hz in real-world scenarios, where the sequential reconstruction approach fails.

In time-decoding based sequential reconstruction (**TDM**), we use matrix pencil [22], [23] for spectral estimation. We use $\widetilde{g}$ ($\widetilde{f}_k$) and $\bar{g}$ ($\bar{f}_k$) to denote the signal recovery (frequency estimate)

TABLE I
NUMERICAL AND HARDWARE EXPERIMENTAL PARAMETERS AND PERFORMANCE EVALUATION.

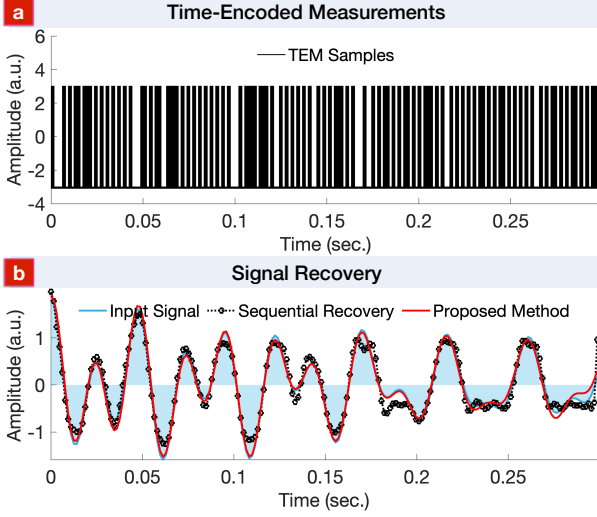| Figure	N	f_s (ED-Prony)	$\bar{f}_s$ (TDM)	$\kappa \times 10^{-4}$	δ	b	$\|g\|_\infty$	f_k	$\widetilde{f}_k$ (ED-Prony)	$\bar{f}_k$ (TDM)	$\mathcal{E}_2\big(\mathbf{f}_k,\widetilde{\mathbf{f}}_k\big)$	$\mathcal{E}_2\big(\mathbf{f}_k,\bar{\mathbf{f}}_k\big)$	$\mathcal{E}_2(\mathbf{g},\widetilde{\mathbf{g}})$	$\mathcal{E}_2(\mathbf{g},\bar{\mathbf{g}})$
		(kHz)	(kHz)					(Hz)	(Hz)	(Hz)				
							Numerical Experiments							
Fig. 2	561	3.50	7.00	4.38	1.50	3.00	1.80	[23.0, 40.0, 42.0]	[23.29, 40.41, 41.80]	[22.95, 41.56, 56.10]	9.71×10^{-2}	6.71×10^{1}	6.68×10^{-3}	3.30×10^{-2}
—	813	6.00	6.00	4.38	1.50	3.50	2.29	[19.0, 20.0, 29.0]	[18.56, 19.84, 29.04]	[19.65, 29.02, 38.55]	7.37×10^{-2}	5.76×10^{1}	2.06×10^{-3}	2.66×10^{-2}
—	853	80.00	400.00	4.38	1.50	3.10	1.90	[8.0, 26.7, 27.0]	[8.01, 26.59, 26.97]	[8.00, 26.81, 26.90]	4.20×10^{-3}	7.25×10^{-3}	1.17×10^{-5}	7.09×10^{-6}
							Hardware Experiments							
—	3116	10.00	100.00	3.82	0.95	4.27	1.51	[49.0, 59.0, 69.0]	[49.10, 59.01, 68.93]	[27.98, 57.88, 72.89]	4.88×10^{-3}	1.53×10^{2}	6.68×10^{-5}	1.29×10^{-3}
—	3055	10.00	100.00	3.48	0.95	4.35	1.53	[54.0, 59.0, 64.0]	[54.01, 58.97, 64.01]	[0.00, 58.40, 69.67]	3.06×10^{-4}	9.83×10^{2}	5.06×10^{-5}	6.44×10^{-4}
Fig. 3	3078	10.00	100.00	3.52	0.95	4.20	1.51	[57.0, 59.0, 61.0]	[56.70, 59.13, 61.04]	[0.00, 58.77, 138.93]	3.68×10^{-2}	3.11×10^{3}	5.22×10^{-5}	7.68×10^{-4}

Fig. 2. Numerical Experiment: (a) Time sequence and (b) signal recoveries. The ground-truth frequencies are $f_k = [23, 40, 42]$Hz. The sequential reconstruction is sensitive to time quantization, while ED-Prony is robust to super-resolve frequency separation of 2 Hz.
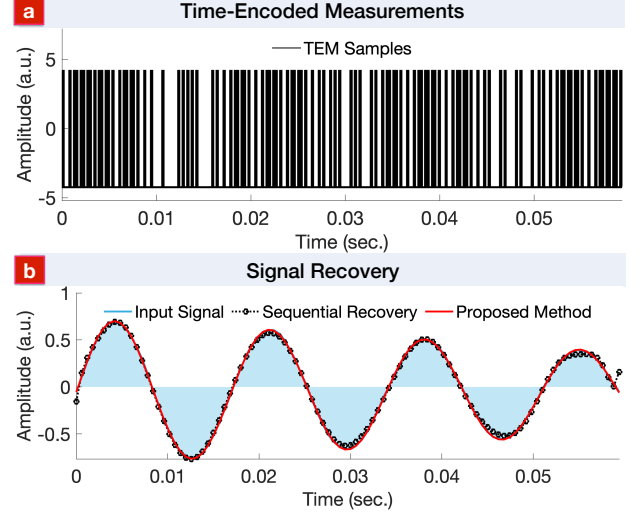

Fig. 3. Hardware Experiment: (a) Time sequence and (b) signal recoveries. The ground-truth frequencies are $f_k = [57, 59, 61]$ Hz. Despite $10\times$ downsampling, ED-Prony super-resolves frequency separation up to a resolution of 2 Hz, where the sequential reconstruction fails.

by Event-Prony (ED-Prony) and sequential reconstruction (TDM) methods, respectively. We use the mean-squared error, defined as $\mathcal{E}_2\big(\mathbf{f}_k,\widetilde{\mathbf{f}}_k\big) = \frac{1}{K}\sum_{k=0}^{K-1}|f_k - \widetilde{f}_k|^2$ to assess the frequency estimation error. Similarly, we use $\mathcal{E}_2(\mathbf{g},\widetilde{\mathbf{g}}) = \frac{1}{M}\sum_{m=0}^{M-1}|g(mT) - \widetilde{g}(mT)|^2$ $(T < \pi/\Omega)$ to measure signal recovery error. Experimental parameters such as, ground-truth frequencies f_k, dynamic range $\|f\|_\infty$, sampling rate (ED-Prony: f_s, sequential reconstruction: $\bar{f}_s$), bias b, among others are tabulated in the first row of Table I, respectively.

Numerical Experiments. We conduct three experiments to validate the super-resolution capacity of ED-Prony: we gradually reduce the minimum frequency separation from 2 Hz to 0.3 Hz. As outlined in Table I, the sequential reconstruction approach is sensitive to quantization on trigger time sequence, resulting in distortion in signal reconstruction as well as the subsequent spectral estimation (see Fig. 2 (b)). Utilizing a robust estimation method, ED-Prony successfully super-resolve closely-located frequencies in all scenarios.

Hardware Experiments. We further conduct three hardware experiments to show the practicability and robustness of ED-Prony algorithm in real-world scenarios. We build EDS hardware based on asynchronous sigma–delta modulator that implements the sampling pipeline depicted in Fig. 1 (b). The input signal $f(t)$ is generated by TG5011A signal generators via amplitude modulation (AM). The experimental parameters and results are tabulated in Table I.

In each experiment, we keep the center frequency (i.e. 59 Hz) fixed and vary frequency separation from 10 Hz to 2 Hz to test the limits of our ED-Prony algorithm. As illustrated in Fig. 3 (b), the sequential reconstruction encounters bottleneck of spectral resolution, due to reconstruction distortion arising from time quantization on $\{t_n\}_{n\in\mathbb{I}_{N+1}}$. As a result, only one frequency component is retrieved by the sequential method and the rest are deviated. Leveraging a *coarse-to-fine* sparse recovery strategy, the proposed ED-Prony algorithm achieves accurate frequency estimation in all challenging scenarios as outlined in Table I, despite the lower sampling rate on trigger times. This effectively corroborates the practical utility and super-resolution capability of the ED-Prony method in various real-world applications.

V. CONCLUSION

Event-driven sampling (EDS) is an alternative paradigm to the Shannon-Nyquist sampling framework, which converts amplitude information into a sequence of non-uniform time stamps. In this paper, we focus on the sum of sinusoids (SoS) signals and design a novel algorithm that enables robust and super-resolved spectral estimation directly from its time-encoded measurements. This method is robust to quantization on trigger times and offers a high-resolution spectral estimation. We go beyond numerical experiments and also provide comprehensive hardware validations of our approach, thus bridging the gap between theory and practice, while showcasing the potential benefits of our method. This also unlocks new opportunities for extending ED-Prony to one-bit sampling applications, such as EDS DOA estimation and radar tracking.

REFERENCES

[1] C. Shannon, "Communication in the presence of noise," *Proc. IRE*, vol. 37, no. 1, pp. 10–21, Jan. 1949.

[2] Y. Tsividis, "Event-driven data acquisition and digital signal processing—a tutorial," *IEEE Transactions on Circuits and Systems II: Express Briefs*, vol. 57, no. 8, pp. 577–581, Aug. 2010.

[3] A. Lazar and L. Toth, "Perfect recovery and sensitivity analysis of time encoded bandlimited signals," *IEEE Trans. Circuits Syst. I*, vol. 51, no. 10, pp. 2060–2073, Oct. 2004.

[4] K. Adam, A. Scholefield, and M. Vetterli, "Sampling and reconstruction of bandlimited signals with multi-channel time encoding," *IEEE Trans. Sig. Proc.*, vol. 68, pp. 1105–1119, 2020.

[5] J. Das and P. Sharma, "Some asynchronous pulse-modulation systems," *Electron Lett*, vol. 3, no. 6, p. 284, 1967.

[6] T. Hawkes and P. Simonpieri, "Signal coding using asynchronous delta modulation," *IEEE Trans. Commun.*, vol. 22, no. 5, pp. 729–731, May 1974.

[7] A. M. Bruckstein and Y. Y. Zeevi, "Analysis of "integrate-to-threshold" neural coding schemes," *Biol. Cybernet.*, vol. 34, no. 2, pp. 63–79, 1979.

[8] E. Roza, "Analog-to-digital conversion via duty-cycle modulation," *IEEE Trans. Circuits Syst. II*, vol. 44, no. 11, pp. 907–914, 1997.

[9] H. G. Feichtinger and K. Gröchenig, "Irregular sampling theorems and series expansions of band-limited functions," *J. Math. Anal. Appl.*, vol. 167, no. 2, pp. 530–556, Jul. 1992.

[10] K. Gröchenig, "A discrete theory of irregular sampling," *Linear Algebra Appl*, vol. 193, pp. 129–150, Nov. 1993.

[11] M. Miskowicz, "Send-on-delta concept: An event-based data reporting strategy," *Sensors*, vol. 6, no. 1, pp. 49–63, Jan. 2006.

[12] B. A. Moser and M. Lunglmayr, "On quasi-isometry of threshold-based sampling," *IEEE Trans. Sig. Proc.*, vol. 67, no. 14, pp. 3832–3841, Jul. 2019.

[13] A. Can, E. Sejdić, and L. Chaparro, "Asynchronous sampling and reconstruction of sparse signals," in *Proc. of the European Sig. Proc. Conf. (EUSIPCO)*, 2012.

[14] R. Alexandru and P. L. Dragotti, "Reconstructing classes of non-bandlimited signals from time encoded information," *IEEE Trans. Sig. Proc.*, vol. 68, pp. 747–763, 2020.

[15] S. Rudresh, A. J. Kamath, and C. Sekhar Seelamantula, "A time-based sampling framework for Finite-Rate-of-Innovation signals," in *Proc. IEEE Int. Conf. Acoust., Speech, Sig. Proc.*, May 2020.

[16] H. Naaman, S. Mulleti, and Y. C. Eldar, "FRI-TEM: Time encoding sampling of finite-rate-of-innovation signals," *IEEE Trans. Sig. Proc.*, vol. 70, pp. 2267–2279, 2022.

[17] G. du Prony, "Essai experimental et analytique sur les lois de la dilatabilite de fluides elastiques et sur celles da la force expansion de la vapeur de l'alcool, a differentes temperatures," *Journal de l'Ecole Polytechnique*, vol. 1, no. 22, pp. 24–76, 1795.

[18] V. F. Pisarenko, "The retrieval of harmonics from a covariance function," *Geophysical Journal International*, vol. 33, no. 3, pp. 347–366, Sep. 1973.

[19] S. Kay and S. Marple, "Spectrum analysis—a modern perspective," *Proc. IEEE*, vol. 69, no. 11, pp. 1380–1419, 1981.

[20] J. Cadzow, "Signal enhancement-a composite property mapping algorithm," *IEEE Trans. Acoust., Speech, Signal Process.*, vol. 36, no. 1, pp. 49–62, 1988.

[21] R. Roy and T. Kailath, "Esprit-estimation of signal parameters via rotational invariance techniques," *IEEE Trans. Acoust., Speech, Signal Process.*, vol. 37, no. 7, pp. 984–995, Jul. 1989.

[22] Y. Hua and T. Sarkar, "Matrix pencil method for estimating parameters of exponentially damped/undamped sinusoids in noise," *IEEE Trans. Acoust., Speech, Signal Process.*, vol. 38, no. 5, pp. 814–824, May 1990.

[23] T. Sarkar and O. Pereira, "Using the matrix pencil method to estimate the parameters of a sum of complex exponentials," *IEEE Antennas Propag. Mag.*, vol. 37, no. 1, pp. 48–55, Feb. 1995.

[24] D. Florescu and A. Bhandari, "Time encoding of sparse signals with flexible filters," in *Intl. Conf. on Sampling Theory and Applications (SampTA)*. IEEE, Jul. 2023.

[25] O. Bar-Shalom and A. Weiss, "DOA estimation using one-bit quantized measurements," *IEEE Trans. Aerosp. Electron. Syst.*, vol. 38, no. 3, pp. 868–884, Jul. 2002.

[26] P. Stoica and R. L. Moses, *Spectral analysis of signals*, 1st ed. Pearson Prentice Hall, 2005.

[27] Y. Li, R. Guo, T. Blu, and H. Zhao, "Generic FRI-based DOA estimation: A model-fitting method," *IEEE Trans. Sig. Proc.*, vol. 69, pp. 4102–4115, 2021.

[28] R. Guo, Y. Li, T. Blu, and H. Zhao, "Vector-FRI recovery of multi-sensor measurements," *IEEE Trans. Sig. Proc.*, vol. 70, pp. 4369–4380, 2022.

[29] V. G. Karmanov, *Mathematical programming*. Mir Publishers, 1989.